MATHEMATICAL MODELING OF THE INTERACTION OF NON-UNIFORM FIELD ACFM WITH FINITE SIZE CRACKS

R. Mostafavi and D. Mirshekar-Syahkal

Department of Electronic Systems Engineering
University of Essex, Colchester CO4 3SQ, UK

INTRODUCTION

The non-destructive evaluation (NDE) of metal surfaces can be accomplished using the alternating current field measurement (ACFM) technique [1]. In this technique a thin-skin eddy current is induced in the metal and the magnetic field above the metal surface is monitored for any perturbation caused by surface defects. In the non-uniform ACFM, the incident field may be produced by a coil or a wire loop carrying a high frequency current [2].

The prediction of the perturbations in the induced current (and hence in the resulting field) by a surface crack, can be made using the finite element or finite difference methods [3]-[4]. These solutions are general and independent of the type of the current distribution in the metal. For this reason, in the limiting case of thin skin eddy current, they are slow computationally. This is due to the fine discretization required for the whole or part of the conductor space.

In a previous paper, we have presented an efficient mathematical technique for the analysis of the interaction of a non-uniform field ACFM with a long uniform crack [5]. Its high efficiency is mainly due to the implementation of the thin skin current assumption in the formulation which leads to an approximate boundary condition at the metal-air interface [1]. The boundary condition is a second-order differential equation in terms of the incident and scattered scalar magnetic potentials. This paper deals with the extension of the technique incorporating a finite length crack with a rectangular shape. The assumed shape is a good approximation to the profiles of some fatigue cracks and it facilitates the development of formulations. The mathematical technique does not depend on the shape of the interrogating field, although in the example given, the incident field is produced by a current-carrying rectangular coil. The mathematical modelling presented can deal with both open and closed cracks. Numerical solution of the problem is achieved by using a two-dimensional Fourier transform, together with the Fourier domain scalar magnetic potentials and the point-matching technique at the lip of the crack. Based on the solution, we have developed a computer program which can predict the field distribution and if required, the crack signal. The accuracy of the method is verified by comparing the predicted and the experimental results.

THEORY

Fig.1.a shows the schematic diagram of the problem. As mentioned earlier, the mathematical modeling has been simplified by exploiting the skin depth. In the case of a very small skin depth, the

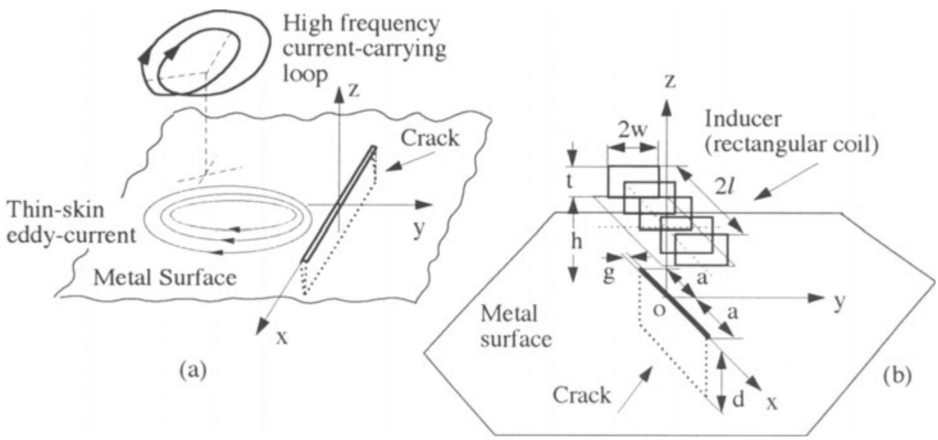

Fig.1 (a) A high frequency current-carrying coil producing a thin skin eddy current around a surface crack in metal and (b) a rectangular inducer symmetrically positioned above a crack with a rectangular boundary.

field inside the metal, including in the region around the crack, can be assumed to decay exponentially. This assumption, coupled with the conservation of magnetic flux at the crack mouth, leads to an approximate boundary condition at the metal surface (z=0) [1];

$$\frac{\mu}{k}\nabla_t^2\psi+\mu_0\frac{\partial\psi}{\partial z}=-(\frac{2\mu}{k}+\mu_0 g)H_z(x,0)\delta(y) \qquad (k=\sqrt{j\omega\mu_0\mu_r\sigma}) \tag{1}$$

where scalar potential ψ represents the sum of the scattered and incident potentials;

$$\psi=\psi_i+\psi_s \tag{2}$$

In (1), g represents the crack opening, $H_z(x,0)=H_z(x,z)|_{z=0}$ is the normal component of the magnetic field distribution at the crack mouth just inside the crack, and other parameters have their usual meaning.

The incident vector magnetic potential for a current- carrying conductor in the air is given by

$$\mathbf{A}_i(r)=\frac{\mu_0}{4\pi}\iiint_{V_0}\frac{\mathbf{J}(r_0)}{|\mathbf{r}-\mathbf{r}_0|}dv_0 \tag{3}$$

Defining a two-dimensional Fourier transform pair;

$$\tilde{\tilde{f}}=\frac{1}{2\pi}\int_{-\infty}^{\infty}\int_{-\infty}^{\infty}fe^{-j(\alpha x+\beta y)}dxdy \tag{4.a}$$

$$f=\frac{1}{2\pi}\int_{-\infty}^{\infty}\int_{-\infty}^{\infty}\tilde{\tilde{f}}e^{j(\alpha x+\beta y)}d\alpha d\beta \tag{4.b}$$

and applying (4.a) to (3) lead to the following expression:

$$\tilde{\tilde{\mathbf{A}}}_i(z) = \frac{\mu_0}{4\pi\gamma} \iiint_{V_0} \mathbf{J}(\mathbf{r}_0) e^{-j(\alpha x_0 + \beta y_0) - \gamma|z - z_0|} dv_0 \tag{5}$$

where $\gamma = \sqrt{\alpha^2 + \beta^2}$. By applying the Fourier transform (4.a) to $\mathbf{B}_i = \nabla \times \mathbf{A}_i$ and $\mathbf{H}_i = -\nabla\psi_i$, and using (5), one obtains

$$\tilde{\tilde{\psi}}_i(z) = \tilde{\tilde{\psi}}_i(0) e^{\gamma z} \qquad z < z_0 \text{ (all points below the inducer)} \tag{6.a}$$

where

$$\tilde{\tilde{\psi}}_i(0) = \frac{1}{j\mu_0\gamma} \mathbf{k} \bullet \vec{\gamma} \times \tilde{\tilde{\mathbf{A}}}_i(0) \tag{6.b}$$

In the above equations $\vec{\gamma} = \alpha\mathbf{i} + \beta\mathbf{j}$ and $\mathbf{i}$, $\mathbf{j}$ and $\mathbf{k}$ are unit vectors in the x, y and z directions. Expressions (6.a) and (6.b) represent the relation between the vector and scalar magnetic potentials at all points below the inducer. From these expressions, it is evident that the incident potential function is a function of vector magnetic potential $\mathbf{A}_i$, and the latter is dependent on the shape of the inducer. For a rectangular coil carrying 1 A current and symmetrically located with respect to the xz and yz planes, Fig.1.b, it can be shown that:

$$\tilde{\tilde{\mathbf{A}}}_i(\alpha,\beta,0) = \frac{\mu_0}{\pi\gamma} \frac{\sin(\alpha l)}{\alpha} \frac{\sin(\beta w)}{\beta} [e^{-\gamma h} - e^{-\gamma(h+t)}](\mathbf{j} - \frac{j\beta}{\gamma}\mathbf{k}) \tag{7}$$

In the above equation, l, w and t are the length, width and the thickness of the rectangular coil respectively. Substituting (7) in (6.b) results in

$$\tilde{\tilde{\psi}}_i(0) = -\frac{j\sin(\alpha l)\sin(\beta w)}{\beta\pi\gamma^2} [e^{-\gamma h} - e^{-\gamma(h+t)}] \tag{8}$$

Since the potential function for the scattered field above the metal surface satisfies Laplace's equation, its general solution in the Fourier domain is given by:

$$\psi_s(z) = a\, e^{-\gamma z} \tag{9}$$

Inserting (9) and (6.a) in (2), the total potential can be written as:

$$\tilde{\tilde{\psi}}(z) = \tilde{\tilde{\psi}}_i(0) e^{\gamma z} + a\, e^{-\gamma z} \tag{10}$$

where a is unknown. Parameter a can be found by combining (10) with the Fourier domain form of the boundary condition, (1). This result can then be used in (10) to obtain the expression for the total potential function at the metal surface;

$$\tilde{\tilde{\psi}}(0) = \frac{2\gamma\mu_0 \tilde{\tilde{\psi}}_i(0) + (\frac{2\mu}{k} + \mu_0 g)\tilde{H}_z(\alpha,0)}{\gamma(\mu_0 + \frac{\mu}{k}\gamma)} \tag{11}$$

Hence, the total potential above the metal surface in the Fourier domain can be expressed as

$$\tilde{\tilde{\psi}}(z)=2\tilde{\tilde{\psi}}_i(0)\frac{\cosh(\gamma z)+\frac{\mu_r\gamma}{k}\sinh(\gamma z)}{1+\frac{\mu_r}{k}\gamma}+(\frac{2\mu_r}{k}+g)\frac{\tilde{H}_z(\alpha,0)}{\gamma(1+\frac{\mu_r}{k}\gamma)}e^{-\gamma z} \tag{12}$$

To find ψ and therefore all the field components in the space domain, the inverse Fourier transform (4.b) has to be applied to (12). However, $\tilde{H}_z(\alpha,0)$ is yet unknown and can be determined as follows.

Inside the crack, the magnetic field can be found from a scalar function ϕ ($\mathbf{H}=-\nabla\phi$) which is the solution of Laplace's equation;

$$\frac{\partial^2\phi}{\partial x^2}+\frac{\partial^2\phi}{\partial z^2}=0 \tag{13}$$

Since the crack is assumed to have a rectangular boundary, Fig.1.b, the scalar function in (13) must meet the following boundary conditions:

$$\frac{\partial\phi}{\partial x}\Big|_{x=\pm a}=0 \quad \text{and} \quad \frac{\partial\phi}{\partial z}\Big|_{z=-d}=0 \tag{14}$$

Hence, the solution to (13) is given by

$$\phi(x,\ z)=\sum_{n=0}^{\infty}C_n\cos\alpha_n(x+a)\frac{\cosh\alpha_n(z+d)}{\cosh(\alpha_n d)} \quad \text{where } \alpha_n=\frac{n\pi}{2a} \tag{15}$$

Using (15), magnetic field component $H_z(x,z)$ inside the crack can be obtained. At the crack mouth (z=0), the Fourier transform of this component with respect to variable x is given by

$$\tilde{H}_z(\alpha,\ 0)=-\frac{1}{\sqrt{2\pi}}\sum_{n=0}^{\infty}C_n\alpha_n\tanh(\alpha_n d)(\frac{j\alpha}{\alpha^2-\alpha_n^2})[e^{-j\alpha a}\cos(n\pi)-e^{j\alpha a}] \tag{16}$$

which is the desired expression for (12). However, in (16) coefficients C_n are yet unknown. They can be computed by using the continuity of potentials ψ and ϕ at the crack mouth;

$$\psi(x,0,0)=\phi(x,0) \qquad |x|\le a \tag{17}$$

and applying the collocation (point matching) technique [6]. In this technique, the number of coefficients to be found is equal to the number of points matched along the crack mouth.

RESULTS

Based on the preceding formulation, a computer program has been developed which uses the fast Fourier transform (FFT). To save time in the computation, the point matching technique is applied at the FFT sampled points. The program produces the magnitude and the phase of the three components of the field resulting from the interaction of a rectangular inducer with a rectangular crack.

In Fig.2, the dimensions of a rectangular inducer and its relative position with respect to a

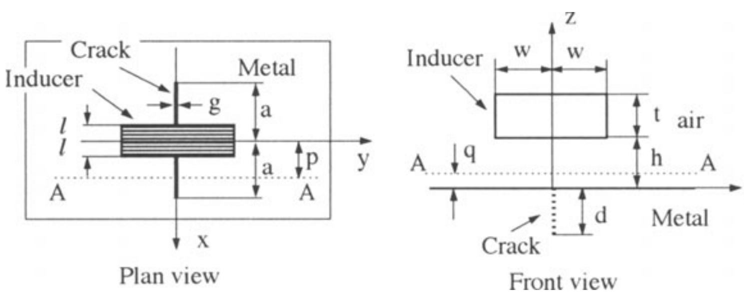

Fig.2 The plan view and front view of a rectangular coil symmetrically located above a crack with a rectangular boundary; l=5 mm, w=10.5 mm, t=4 mm, a=10 mm, d=4 mm, g=0.1 mm, h=3.7 mm, q=0.84 mm and p=6.7 mm.

rectangular crack, are shown. In the absence of the crack, the magnitude and phase of the y component of the field produced by the inducer at a distance of q=0.84 mm above the metal surface were computed and are depicted in Fig.3.a and 3.b. This component (H_y) plays an important role in the high sensitivity ACFM [2]. If required, the phases and magnitudes of the other two components of the field can also be computed. To validate the computed results, those corresponding to line AA in Fig.2 are compared with the measurement results, Figs.3.c and 3.d. A similar set of results in the presence of the crack, are presented in Fig.4. It should be noted that in the measurement, an arc-circular crack with a $\approx$ 18 mm, d $\approx$ 5 mm and g $\approx$ 0.1 mm was used whose depth below line AA is about 4 mm. As Figs.4.c and 4.d show, in spite of the difference in the shapes of the crack and the notch, the experimental and theoretical results are in very good agreement. This is because line AA is not near a crack end. In Figs.3.b, 3.d, 4.b and 4.d for the phase, the well-known Gibb's phenomenon (associated with Fourier transform of discontinuous functions) is discernible in the theoretical results. Also, the experimental results for the phase at discontinuities suffer from the finite time-constant

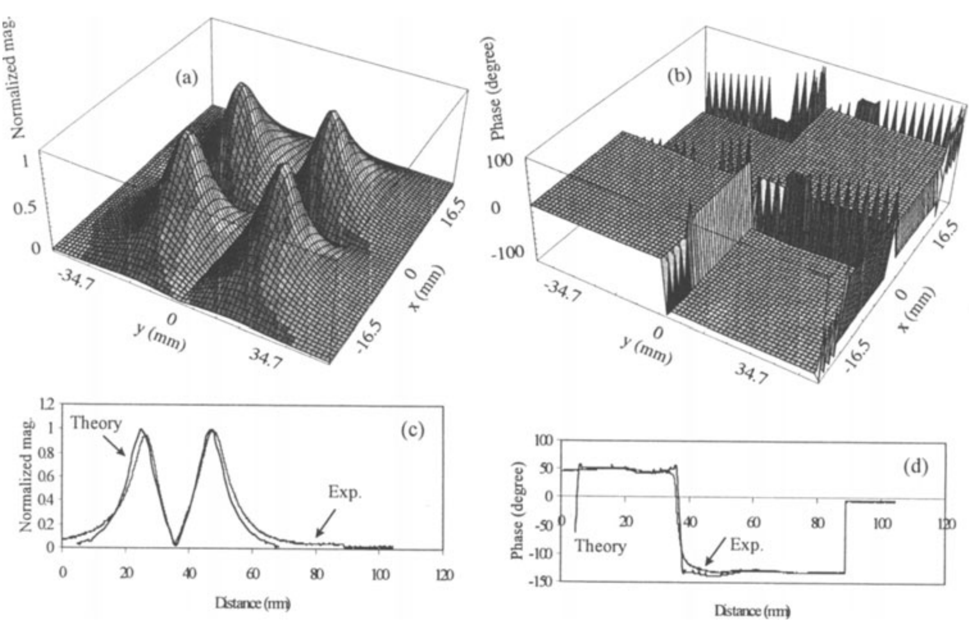

Fig.3 (a) Normalized magnitude and (b) phase of H_y at distance q=0.84 mm above mild steel in the absence of the crack. (c) Normalized magnitude and (d) phase along line AA shown in Fig.2.

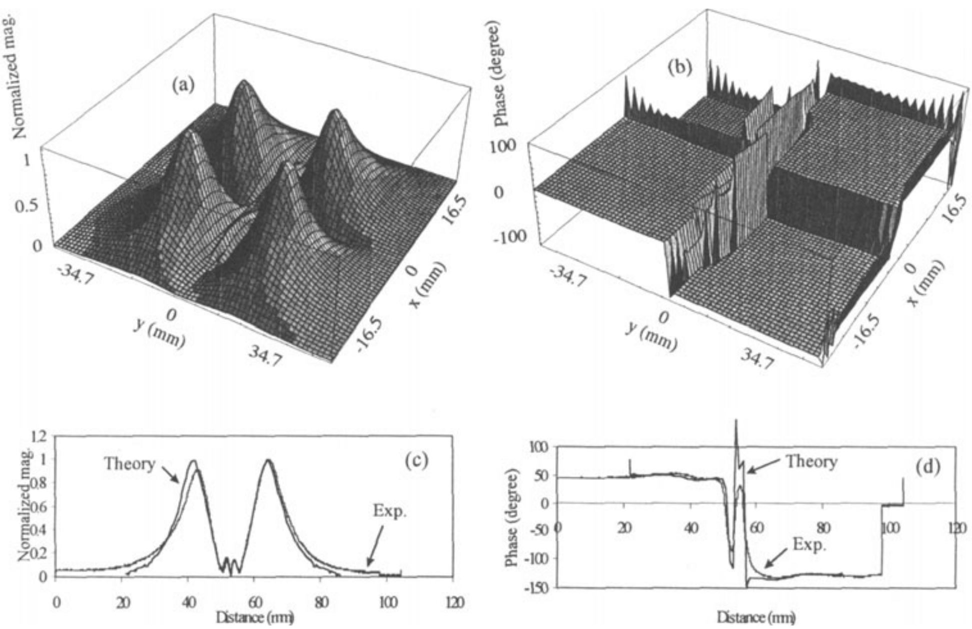

Fig.4 (a) Normalized magnitude and (b) phase of H_y at distance q=0.84 mm above mild steel in the presence of the rectangular crack, Fig.2. (c) Normalized magnitude and (d) phase along line AA shown in Fig.2.

effect of the phase channel of the phase-lock detector system used for the measurement. This effect smoothes the edges and reduces the phase shift at discontinuities, Figs.3 and 4.

CONCLUSION

An accurate mathematical technique for the analysis of the interaction of a non-uniform field ACFM with open and closed rectangular cracks, was presented. The assumed shape is a good approximation to the profile of some cracks. The technique is efficient computationally which is mainly due to the implementation of the assumption of the thin skin current in the formulation, leading to an approximate, but convenient boundary condition at the metal-air interface. For the computation, it employs a two-dimensional Fourier transform, together with the Fourier domain scalar magnetic potentials and the point-matching technique at the lip of the crack. In the technique presented, the interrogating field can have an arbitrary shape. However, in the example treated in this paper, the incident field is due to a current-carrying rectangular coil. The accuracy of the method was verified by comparing the computed and measured results.

REFERENCES

1. D. H. Michael, A. M. Lewis, M. McIver and R. Collins, Proc. R. Soc. Lond., A434, (1991), p. 587.
2. D. Mirshekar-Syahkal and R. F. Mostafavi, in *Review of Progress in QNDE*, eds. D. O. Thompson and D. E. Chimenti (Plenum Press, New York, 1996), Vol. 15A, p. 1121.
3. 3.R. Ludwig and X. Dai, IEEE Trans. Magn., 26, (1990), p. 299.
4. J. A. Krawczyk and J. A. Tegopoulos, *Numerical Modelling of Eddy Currents* (Claredon Press, Oxford, 1993).
5. D. Mirshekar-Syahkal and R. F. Mostafavi, IEEE Trans. Magn., 33, (1997), p. 2291.
6. R. H. T. Bates, IEEE Trans. Microwave Theory Tech., 15, (1967), p. 185.